




Cite this: *RSC Adv.*, 2017, 7, 39270

# Novel sulfonate-containing halogen-free flame-retardants: effect of ternary and quaternary sulfonates centered on adamantane on the properties of polycarbonate composites†

Dong Yu Zhu,  Jian Wei Guo,\* Jia Xing Xian and Shu Qin Fu

In order to find a more environmentally friendly flame retardant, we have designed a novel halogen-free flame-retardant (FR) system consisting of ternary and quaternary sulfonates centered on adamantane. They are named 1,3,5-tri(phenyl-4-sodium sulfonate)adamantane (AS<sub>3</sub>) and 1,3,5,7-tetrakis(phenyl-4-sodium sulfonate)adamantane (AS<sub>4</sub>), respectively. Both kinds of FRs were synthesized and compounded with polycarbonate (PC) to study their effects on the properties of PC composites. The results show that the new FR system can improve PC flame retardancy efficiently, and has mechanical strength advantages as well. The PC composites with only 0.1 wt% AS<sub>3</sub> or 0.08 wt% AS<sub>4</sub> can pass vertical burning tests (UL-94) V-0 level, with increasing the value of limiting oxygen index (LOI) to 31.2% or 32.3%. Moreover, they can maintain ideal mechanical properties compared to neat PC simultaneously. Finally, the flame retardant mechanism of this system was verified *via* thermal analysis, morphology and chemical structure analysis of the char residues.

Received 12th June 2017  
Accepted 3rd July 2017

DOI: 10.1039/c7ra06504c

rsc.li/rsc-advances

## 1 Introduction

With the development of technology, polymer materials are used with an ever increasing magnitude instead of metal or ceramics in all kinds of areas. However, fire hazards associated with the use of these polymeric materials are usually present and can cause heavy loss of life and property.<sup>1–3</sup> Therefore, it is vital to reduce the combustibility of the polymers by using flame retardants in the development and application of new materials.<sup>4</sup> Polycarbonate (PC) is one of the fastest growing engineering plastics containing excellent physical properties including transparency, toughness, high heat distortion temperature, and beneficial mechanical properties.<sup>5</sup> Generally, PC shows a V-2 rating in the UL-94 test and the oxygen index is about 25%, but it is still difficult to meet the needs of more stringent flame retardant performance in many practical applications.<sup>6–8</sup>

For the sake of safety, all kinds of flame retardants have been developed and used for PC. The halogen-containing flame-retardants that have high flame-resistant efficiency, however, have been gradually forbidden due to the generated toxicity and environmental problems. Because of this, the development of environmentally friendly halogen-free flame retardants has

attracted the interests of more and more researchers from both the academic and industrial fields.<sup>9–15</sup> However, the general non-halogenated flame retardants (FR) such as phosphorus-, silicon-, and nitrogen-containing FRs are usually not efficient enough to enable PC to pass V-0 rating in the UL 94 test until being incorporated with a relatively large amount.<sup>6,16–20</sup> For example, among the above halogen-free FRs, phosphorus-containing compounds like triphenyl phosphate (TPP) and resorcinol bis(diphenyl phosphate) (RDP) are the most widely used FRs for PC and their blends, but generally, to enable PC passing UL94 V-0 test, the required additive amount should be as much as 5–15 wt%.<sup>21–25</sup> As we known, the additive type flame retardants are generally incorporated into polymeric materials by physical means, a large amount of addition may bring in a variety of problems, such as poor transparency, leaching, and a reduction in mechanical properties.

According to the study,<sup>26–28</sup> organosulfonates such as the commercially available potassium diphenylsulfone sulfonate (KSS) are highly effective FRs for PC. In general, very low additions (no less than 1 wt%) of certain metal salt sulfonates can provide a self-extinguishing performance to polycarbonate. However, the halogen-free flame retarding PC composites incorporated with current sulfonates FRs like KSS still have drawbacks. For example, higher flame retardancy is limited and the mechanical properties suffer a loss, which can be attributed to the poor interfacial adhesion between FR and the polymer matrix. Therefore, to design a series of novel efficient sulfonate FRs and to study the effect of their structure on the properties of

School of Chemical Engineering and Light Industry, Guangdong University of Technology, Guangzhou 510006, China. E-mail: guojw@gdut.edu.cn

† Electronic supplementary information (ESI) available. See DOI: 10.1039/c7ra06504c



PC composites is of great significance for promoting the development of this field.

In this paper, ternary and quaternary sulfonate centered on adamantane were designed as 1,3,5-tri(phenyl-4-sodium sulfonate)adamantane (AS<sub>3</sub>) and 1,3,5,7-tetrakis(phenyl-4-sodium sulfonate)adamantane (AS<sub>4</sub>), respectively. Owing to the various advantages of adamantane such as having stereo-regularity, multiple substitutability, excellent lipophilicity, good thermal and oxidative stabilities and high rigidity, the novel sulfonate flame retardant with high sulfur content is expected to be more efficient for flame retardancy and less negative to mechanical property. In this study, these two kinds of FRs were first synthesized and characterized, then the flammability of PC composites filled with the novel FR were investigated using a cone calorimeter, as well as the LOI and UL-94 tests. The effect of the two kinds of FR content on mechanical properties and thermal properties of PC/AS<sub>n</sub> ( $n = 3, 4$ ) was also systematically studied. Finally, the flame retarding mechanism was deduced from the thermal degradation and the residual char morphology and chemical structure. Using this system, PC composites with only 0.08 wt% AS<sub>4</sub> or 0.1 wt% AS<sub>3</sub> can pass V-0 and have LOI value higher than 30, and can maintain ideal mechanical properties as well. In addition, it is found that the higher the sulfonate content in FR molecular structure, the better for flame retardant PC.

## 2 Experimental

### 2.1 Materials

Polycarbonate (PC, grade: 301-10) was supplied by Dow Chemical Company (American) with a melt index (GB 368283) of 20 g/10 min and a density of 0.918 g cm<sup>-3</sup>. PC was dried in the oven at 120 °C for 8 h prior to blending. Adamantane (99%) was purchased from Zhang jia gang Xikai Chemical Co., Ltd., China. Bromine (AR, 99.5%), Aluminium chloride (AR, 99%) and *tert*-butyl bromide (AR, 99%) were purchased from Aladdin. Chlorosulfonic acid (AR) was supplied by Xiya Reagent Co., Ltd., China. The potassium diphenylsulfone sulfonate (KSS) used here as a reference flame retardant was offered by Guangdong Ever Sun Corp., China. Benzene (AR) and dichloromethane (AR) purchased from Guangzhou Chemical Reagent Factory, were distilled in anhydrous calcium chloride before used. Other chemicals were all used without further purification.

### 2.2 Synthesis of ternary and quaternary sulfonate FR AS<sub>3</sub> and AS<sub>4</sub>

The AS<sub>n</sub> ( $n = 3, 4$ ) was synthesized through the reactions of Friedel-Crafts arylation from 1-bromoadamantane,<sup>29</sup> followed by substitution reaction, hydrolysis reaction and neutralization reaction according to the above reaction route as shown in Scheme 1.

A typical procedure for synthesis of 1,3,5-triphenyladamantane is as follows: 5.0 g 1-bromoadamantane (23 mmol), 6.5 g *tert*-butyl bromide (50 mmol), and 175 mL benzene was introduced into a 500 mL three-neck flask equipped with a reflux condenser, a calcium chloride drying tube and

a magnetic stirrer. After being stirred for 10 min at 55 °C, 0.2 g aluminium chloride (1.9 mmol) was added slowly and the reaction solution was heated under vigorous reflux for another 10 minutes. Finally, the system was then poured into an ice water and ether mixture, the resultant undissolved substance was filtrated and extracted by chloroform, followed by recrystallization from benzene to get the final product of 1,3,5-triphenyladamantane.

The procedure for preparing 1,3,5,7-tetraphenyladamantane is very similar to that for 1,3,5-triphenyladamantane, except for using more catalyst of aluminium chloride (0.6 g) and reacting for a longer time of 60 min in the same case as shown above. In addition, after the reaction completed, the product is insoluble, so it should be obtained as the filter residue not the filtrate after Soxhlet extraction from chloroform. Finally, 1,3,5,7-tetraphenyladamantane was gained after vacuum dried as white solid.

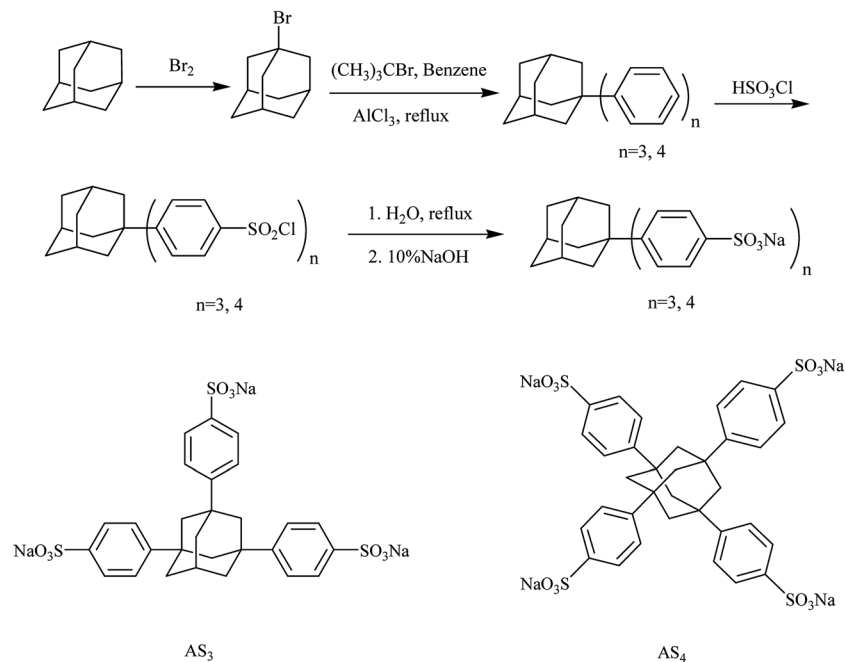
The reaction approaches for both 1,3,5-tri(phenyl-4-sulfochloride)adamantane and 1,3,5,7-tetrakis(phenyl-4-sulfochloride)adamantane are the same. Take 1,3,5-tri(phenyl-4-sulfochloride)adamantane for example, a typical procedure is as follows: 1.35 g 1,3,5-triphenyladamantane (3.72 mmol), 20 mL dry dichloromethane was added to a 100 mL three-neck flask equipped with a reflux condenser, a calcium chloride drying tube, a dropping funnel and a magnetic stirrer in an ice bath, and then to the reaction system was dropwise added 2.5 mL chlorosulfonic acid and 5 mL dichloromethane within 10 min. The temperature was slowly raised to 35 °C and kept stirring for 75 min. After cooling to room temperature, the organic layer was separated by centrifuge, and rotary evaporated to get a brown oil which was washed by water and then filtrated. Finally, 2.35 g (95.7%) solid product of 1,3,5-tri(phenyl-4-sulfochloride)adamantane was obtained after vacuum dried at 45 °C for 12 h.

The procedure for the final step is the same for both AS<sub>3</sub> and AS<sub>4</sub>. To take AS<sub>3</sub> for example, a typical method is as follows: 5.0 g 1,3,5-tri(phenyl-4-sulfochloride)adamantane and 300 mL deionized water was added to a 500 mL flask with a reflux condenser and a magnetic stirrer. The mixture was heated at 100 °C for 24 h to give a clear solution which was distilled under reduced pressure, and the residue was dried by vacuum oven at 45 °C for 12 h. Next, the resultant solid was dissolved in 50 mL of water and was neutralized by 10 wt% NaOH solution. After the water was thoroughly removed, the residue was bleached and vacuum dried to afford 5.0 g (98.4%) the product of AS<sub>3</sub> as a white salt.

### 2.3 Preparation of flame retardant PC composites

PC and the flame retardants AS<sub>3</sub> and AS<sub>4</sub> were first dried overnight at 120 °C before compounding. The PC composites filled with 0.06–0.16 wt% AS<sub>3</sub> or AS<sub>4</sub> FR were prepared in a HL-200 internal mixer (Jilin University Science and Education Instrument factory, China) under 50 rpm for 8 min at the temperature of 245 °C, which were denoted as PC/AS<sub>3</sub> (0.06%), PC/AS<sub>3</sub> (0.08%), PC/AS<sub>3</sub> (0.1%), PC/AS<sub>3</sub> (0.12%), and PC/AS<sub>3</sub> (0.16%), respectively. PC/AS<sub>4</sub> were labeled in the same manner. The compounds were then broken into pieces and dried in a vacuum





Scheme 1 Synthesis route and structures of flame retardants  $AS_n$  ( $n = 3, 4$ ).

oven at 90 °C over 5 h. Afterwards, the composite pieces were injection molded or compression molded into standard sizes for different tests. Unfilled PC and the PC composites filled with flame retardant KSS of a suitable amount were also manufactured under the same conditions for comparison.

## 2.4 Characterization and measurements

**2.4.1 Spectroscopic analysis.** The Fourier transform infrared (FTIR) spectra were recorded with KBr on a Nicolet 6700 FTIR spectrometer from 400 to 4000  $\text{cm}^{-1}$ . The hydrogen nuclear magnetic resonance ( $^1\text{H-NMR}$ ) spectra were recorded on a Bruker AVANCE III HD400-MHz superconducting NMR spectrometer.

**2.4.2 Flammability tests.** Limiting oxygen index (LOI) measurements were carried out using a HP6115 type oxygen index test apparatus (Foshan, China) following an ASTM D2863-2008 standard procedure, and the dimensions of all samples were 80 mm  $\times$  10 mm  $\times$  4 mm. The LOI values were calculated based on the results of five tests.

The vertical burning tests (UL-94) were conducted on a ZRS-2 vertical horizontal burning apparatus (NEARBYMRO, Germany) according to ASTM D3801 standard, the dimensions of all samples were 125 mm  $\times$  13 mm  $\times$  3 mm. In the test, five sample bars suspended vertically over surgical cotton were ignited using a 50 W methane gas burner.

The cone calorimetry test was carried out by using a FTT 0007 cone calorimeter (Fire Testing Technology, UK) in accordance with the ISO 5660 standard procedures. Each specimen, with a dimension of 100 mm  $\times$  100 mm  $\times$  3 mm, was wrapped in aluminum foil and exposed horizontally to an external heat flux of 35  $\text{kW m}^{-2}$ . The recorded parameters included the time to ignition (TTI), heat release rate (HRR,  $\text{kW m}^{-2}$ ), peak value of

the heat release rate (PHRR,  $\text{kW m}^{-2}$ ), specific extinction area (SEA), the peak value of smoke production rate (SPR), and CO production rate (COP).

**2.4.3 Mechanical tests.** The tensile and flexural tests were performed using a PHM-5 universal tester according to an ISO 844 and ASTM D790 standard procedure, respectively. Each batch included five specimens to yield averaged values.

## 2.5 Thermogravimetric analysis and thermal degradation kinetics

Thermogravimetric analysis (TGA) and thermal degradation kinetics were carried out with a NetzschSTA409 PC thermoanalyzer instrument (Netzsch, Germany). For the thermal analysis of FRs, each sample was heated from 50 to 800 °C at the rate of 20 °C  $\text{min}^{-1}$  under nitrogen atmosphere. To test the thermal degradation kinetics, each sample was heated from 50 to 800 °C at various rates of 5, 10, 15 and 20 °C  $\text{min}^{-1}$  under air atmosphere. The Flynn–Wall–Ozawa method was used to analyze the thermal degradation kinetics parameters.

## 2.6 Scanning electron microscopy (SEM)

The SEM observation was performed on a Hitachi S-3400N scanning electron microscope (Hitachi, Japan) to investigate the morphology of the char layer of samples after the LOI tests.

# 3 Results and discussion

## 3.1 Chemical structure characterization of FRs

The flame retardant  $AS_3$  and  $AS_4$  were synthesized *via* the reaction route presented in Scheme 1. The  $^1\text{H}$  NMR, IR spectra and elementary analysis data for each intermediate product were provided in the ESI (Fig. S1–S7†). Fig. 1(a) shows the  $^1\text{H}$



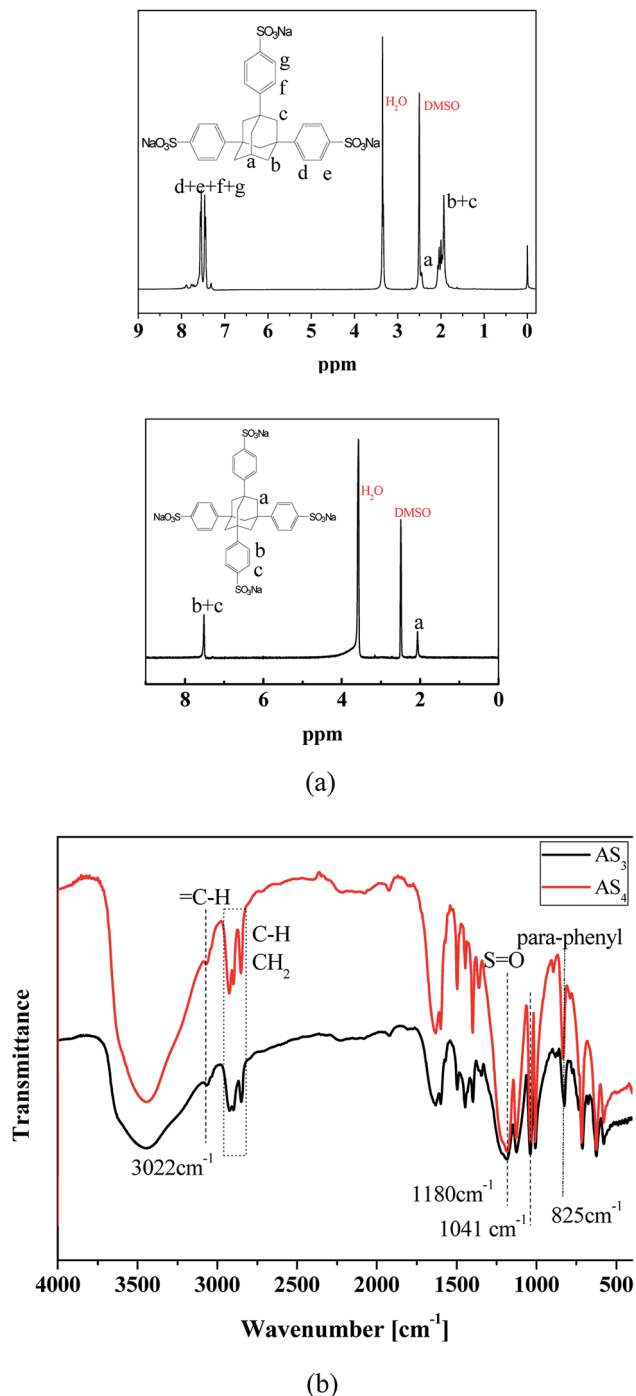


Fig. 1 (a)  $^1\text{H}$  NMR spectra of  $\text{AS}_3$  and  $\text{AS}_4$  with  $\text{DMSO-d}_6$  as solvent, (b) FTIR spectra of  $\text{AS}_3$  and  $\text{AS}_4$ .

NMR spectra of  $\text{AS}_3$  and  $\text{AS}_4$  with  $\text{DMSO-d}_6$  as a solvent, and Fig. 1(b) the IR spectra.

The  $^1\text{H}$  NMR spectrum of  $\text{AS}_3$  is shown in Fig. 1(a), the multi-peaks at 1.932–2.070 ppm (m, 12H) correspond to the protons (b + c) of  $-\text{CH}_2$  in adamantyl. The peak at 2.447 ppm (s, 1H) is attributed to the (a) proton of  $-\text{CH}$  in adamantyl, and the peaks during 7.444–7.564 ppm (m, 12H) are due to (d + e + f + g) protons in the benzene ring.

As shown in the right side of Fig. 1(a) which is the  $^1\text{H}$  NMR spectrum of  $\text{AS}_4$ , we can see the chemical shifts of H protons at the peak appearing at 2.06 (s, 12H) correspond to the H protons (a) in  $\text{CH}_2$  of tetra-substituted adamantyl, and the peaks at 7.515–7.551 (m, 16H) are assigned to H protons (b + c) in  $=\text{C}-\text{H}$  of benzene ring.

To confirm the successful synthesis of  $\text{AS}_3$  and  $\text{AS}_4$ , FT-IR spectra were also recorded and presented in Fig. 1(b).  $\text{AS}_3$  shows almost the same absorption peaks with  $\text{AS}_4$ . The peaks at  $3022\text{ cm}^{-1}$ ,  $1600\text{ cm}^{-1}$  and  $1495\text{ cm}^{-1}$  should be attributed to the stretching vibrations of  $=\text{C}-\text{H}$  and  $\text{C}=\text{C}$  in benzene rings, respectively, and the characteristic absorption peak of *para*-disubstituted benzene ring is observed at  $825\text{ cm}^{-1}$ . The peaks corresponding to stretching vibration and the deformed vibration of  $\text{C}-\text{H}$  and  $-\text{CH}_2$  in adamantane appear at  $2923$ ,  $1446$ ,  $712\text{ cm}^{-1}$ . The characteristic absorption of  $\text{S}=\text{O}$  which belongs to the sulfonate group is observed at  $1180$  and  $1041\text{ cm}^{-1}$ . In addition, it can be also shown that a broad absorption peak appears at  $3444\text{ cm}^{-1}$ , which should correspond to the signal of absorbed water. Conclusively, the  $^1\text{H}$  NMR and the FTIR spectra confirm that  $\text{AS}_3$  and  $\text{AS}_4$  have been synthesized successfully.

### 3.2 Thermal analysis of FRs

The basic thermal properties of FRs are vital for their application in polymers.

Fig. 2 shows the thermal stability of the flame retardant  $\text{AS}_3$  and  $\text{AS}_4$  by thermogravimetric analysis under nitrogen atmosphere. Both  $\text{AS}_3$  and  $\text{AS}_4$  display the similar TG and DTG curves, but  $\text{AS}_4$  has a little higher degradation temperature. As shown in Fig. 2, about 10 wt% weight loss between  $100$  and  $300\text{ }^\circ\text{C}$  results from the evaporation of (i) absorbed moisture and (ii) crystal water. According to the weight loss percent of the corresponding part on the curves, the maximum weight loss between  $480\text{ }^\circ\text{C}$  and  $550\text{ }^\circ\text{C}$  should correspond to the released  $\text{SO}_2$  from the decomposition of the sulfonate groups, and the last stage of weight loss between  $630\text{ }^\circ\text{C}$  and  $800\text{ }^\circ\text{C}$  should be attributed to the pyrolysis of  $-\text{ONa}$  from benzene rings. The residues should be 1,3,5-triphenyladamantane or 1,3,5,7-tetraphenyladamantane and

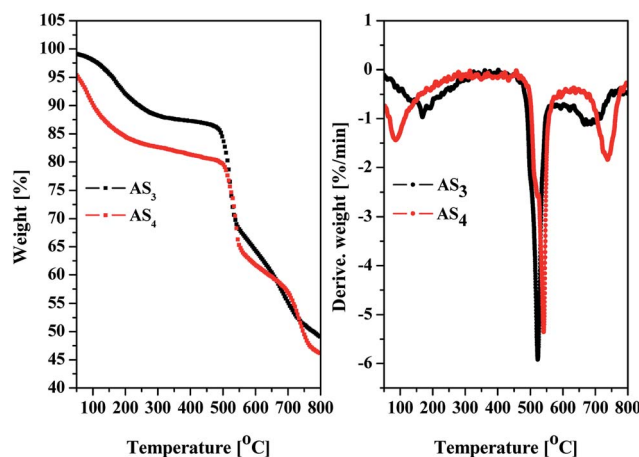


Fig. 2 TG and DTG curves of  $\text{AS}_3$  and  $\text{AS}_4$  recorded in  $\text{N}_2$ .





sodium ions. In general, proper decomposition temperature is very important for additive-type flame retardants to work for matrix materials. The maximum decomposition peak temperature which corresponds to the degradation of sulfonate is 527.7 °C for AS<sub>3</sub> and 543.3 °C for AS<sub>4</sub>, that is much higher than the thermo-processing temperature of PC composites and matchable with the degradation temperature of PC ( $T_{\text{peak}} = 534.2$  °C) (see Fig. 7). It demonstrates that the novel FR system of AS<sub>3</sub> and AS<sub>4</sub> can well meet the demand for flame retardants of PC in regards to thermal property.

### 3.3 Flammability of PC composites

The flammability of PC/AS<sub>*n*</sub> (*n* = 3, 4) composites was systematically evaluated using LOI, UL-94 and cone calorimetry methods. The results of LOI and UL-94 tests for PC/AS<sub>*n*</sub> with different loadings and PC/KSS composites as the control samples are displayed in the above Fig. 3. As shown in Fig. 3, the LOI value of neat PC is 25.8%. After being added with the synthesized new FRs, we can see that both AS<sub>3</sub> and AS<sub>4</sub> improved the flammability of PC composites efficiently. According to the JISK 7201 industrial standard, with LOI >30%, PC/AS<sub>3</sub> with AS<sub>3</sub> content between 0.1–0.16 wt% and PC/AS<sub>4</sub> with AS<sub>4</sub> content 0.08–0.16 wt% within the range studied, can all be assigned to the first class flame retardant materials that are extremely hard to ignite. As to the UL-94 tests, it also can be clearly indicated from Fig. 3 that the UL-94 rating for neat PC is V-2. As to the flame retardant PC composites, only 0.1 wt% AS<sub>3</sub> or even 0.08 wt% AS<sub>4</sub> can enhance PC materials to pass V-0 rating. So the optimal FR addition amount can be 0.1 wt% for AS<sub>3</sub> and 0.08 wt% for AS<sub>4</sub>. In contrast, the control samples, which are added with KSS as FR instead, under the same FR content, can only reach V-2 with the LOI value of 27.1% for PC/KSS (0.08 wt%) and 28.6% for PC/KSS (0.1 wt%), respectively. Thus the above results from both LOI and UL-94 manifest that our synthesized AS<sub>3</sub> or AS<sub>4</sub> indeed works well in flame-retarding of PC composites, and AS<sub>4</sub> which has more sulfonate content in molecular structure is shown more efficient than AS<sub>3</sub>.

Cone calorimetry, as one of the most important bench-scale methods for evaluating the flame retarding performance of materials in a real fire case,<sup>30</sup> was further investigated in this

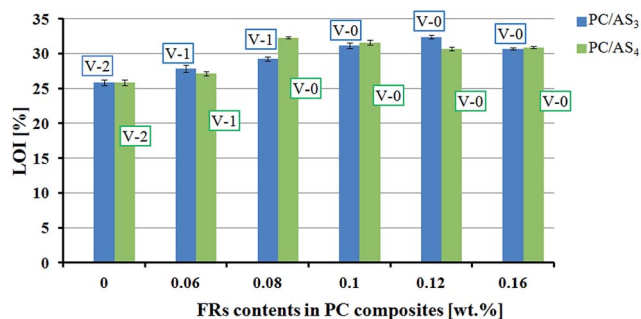


Fig. 3 The LOI values and UL-94 results of flame retardant PC composites PC/AS<sub>3</sub> and PC/AS<sub>4</sub> with different FR contents. For the control sample of PC/KSS (0.08%) is 27.1%, V-2, and PC/KSS (0.1%) 28.6%, V-2.

Table 1 Cone calorimetric data with a heat flux of 35 kW m<sup>-2</sup>

Sample	PC	PC/AS <sub>3</sub> (0.10%)	PC/AS <sub>4</sub> (0.08%)
TTI/s	102	72	86
pHRR (kW m <sup>-2</sup> )	305.9	243.2	247.8
THR (MJ m <sup>-2</sup> )	61.0	53.3	59.4
SEA (m <sup>3</sup> kg <sup>-1</sup> )	680.5	510.3	573.3
pkSPR (m <sup>3</sup> s <sup>-1</sup> )	0.133	0.081	0.079
Mean COY (kg kg <sup>-1</sup> )	0.148	0.103	0.089

work. The samples of PC/AS<sub>3</sub> (0.1%), PC/AS<sub>4</sub> (0.08%) and PC are tested by cone calorimeter and some of the important results are summarized in Table 1. The heat release rate (HRR), in particular the peak of HRR (pHRR) value, is proved to be the most useful parameter to evaluate fire safety. Fig. 4 shows the HRR plots for pure PC, PC/AS<sub>3</sub> (0.1%), and PC/AS<sub>4</sub> (0.08%) composites.

It can be seen from Table 1 and Fig. 4 that neat PC shows a very sharp HRR curve at the time range of 100–400 s with a maximum of 305.9 kW m<sup>-2</sup> at 125 s. In comparison, the HRR curves of PC/AS<sub>3</sub> (0.1%) and PC/AS<sub>4</sub> (0.08%) both become flatter, indicating the lower intensity of a fire. The peak HRR (pHRR) values decrease to 243.2 kW m<sup>-2</sup> and 247.8 kW m<sup>-2</sup> for PC/AS<sub>3</sub> (0.1%) and PC/AS<sub>4</sub> (0.08%), respectively. The total heat release (THR) value for neat PC is 61.0 MJ m<sup>-2</sup>, and it also decreases to 53.3 MJ m<sup>-2</sup> and 59.4 MJ m<sup>-2</sup> for PC/AS<sub>3</sub> (0.1%) and PC/AS<sub>4</sub> (0.08%), respectively. These results demonstrate that both AS<sub>3</sub> and AS<sub>4</sub> can effectively reduce the risk of fire hazard.

Smoke and toxic gas release performances are other very important parameters to determine flame-retardant material in fire safety judgment.<sup>31</sup> As seen in Table 1, the SEA data which measures the total generated smoke quantity decreases from 680.5 m<sup>3</sup> kg<sup>-1</sup> for PC to 510.3 m<sup>3</sup> kg<sup>-1</sup> and 573.3 m<sup>3</sup> kg<sup>-1</sup> for PC/AS<sub>3</sub> (0.1%) and PC/AS<sub>4</sub> (0.08%), respectively. And the pkSPR is also decreased from 0.133 m<sup>3</sup> s<sup>-1</sup> to 0.081 m<sup>3</sup> s<sup>-1</sup> and 0.079 m<sup>3</sup> s<sup>-1</sup>, respectively. The lower value of SEA and pkSPR indicates that AS<sub>3</sub> and AS<sub>4</sub> can both strongly cut down the

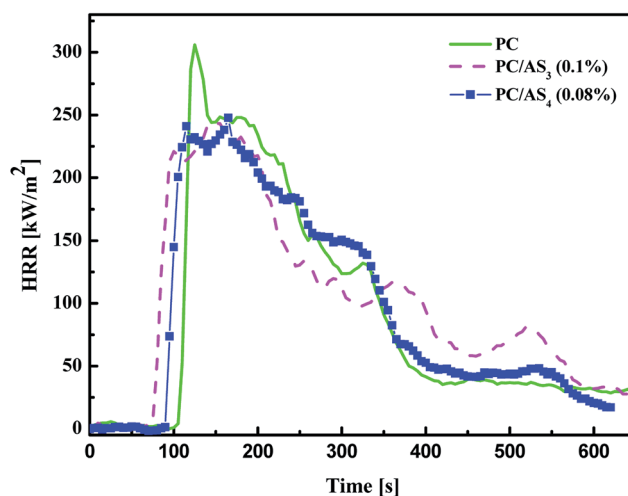


Fig. 4 Heat release rate curves of PC, PC/AS<sub>3</sub> (0.1%) and PC/AS<sub>4</sub> (0.08%) composites.



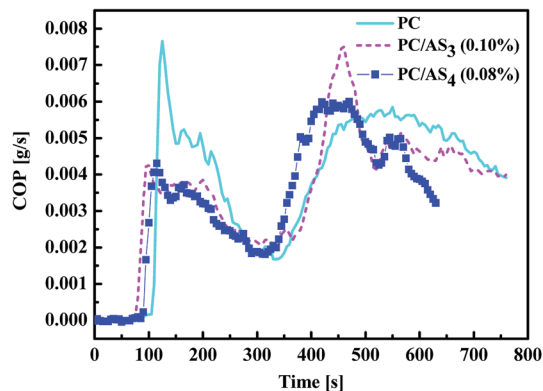


Fig. 5 CO release rate curves of PC, PC/AS<sub>3</sub> (0.1%) and PC/AS<sub>4</sub> (0.08%) composites.

smoke emission of PC composites. Fig. 5 shows the variation of CO production during the combustion process. The mean CO yield of PC is 0.148 kg kg<sup>-1</sup>. With addition of AS<sub>n</sub> ( $n = 3, 4$ ) FR, the mean CO yield decreased to 0.103 kg kg<sup>-1</sup> and 0.089 kg kg<sup>-1</sup> for PC/AS<sub>3</sub> (0.1%) and PC/AS<sub>4</sub> (0.08%), respectively. Moreover, the first peak CO production is significantly decreased from 0.0077 kg kg<sup>-1</sup> for neat PC to 0.0043 kg kg<sup>-1</sup> and 0.0044 kg kg<sup>-1</sup>, respectively. This means that the AS<sub>3</sub> or AS<sub>4</sub> flame retardant system can efficiently suppress poisonous gas emission so as to increase the likelihood of survival at the beginning of a fire.

It is worthwhile to mention that the TTI of pure PC is 102 s, while it is decreased to 72 s and 86 s with addition of 0.1 wt% AS<sub>3</sub> and 0.08 wt% AS<sub>4</sub>, respectively. The unexpected decrease in TTI of PC/AS<sub>n</sub> composites indicates that AS<sub>3</sub> and AS<sub>4</sub> may retard the combustion of PC matrix through accelerating the thermal decomposition of PC and quickly promoting the formation of char layers at relatively lower temperature.

From the LOI test, UL-94 test and cone calorimeter results which are discussed above, it is clear that the flame retardancy of PC is significantly enhanced by incorporation of AS<sub>3</sub> or AS<sub>4</sub> FRs.

### 3.4 Mechanical properties

As an additive-type flame retardant, the effect of its incorporation on the mechanical properties of matrix material is a matter of concern. Fig. 6 depicts the tensile and flexural properties of PC and its composites. As shown in Fig. 6(a), the tensile strength of virgin PC is 60.55 MPa. With increasing of AS<sub>3</sub> content, the tensile strength of PC/AS<sub>3</sub> composites increases first and then levels off after a slight decrease. As to PC/AS<sub>4</sub>, the tensile strength keeps gradually increasing and then levels off with additional AS<sub>4</sub> content. With the addition of FR at the optimal content for flame retardancy, the tensile strength rises to 61.58 MPa and 61.88 MPa for PC/AS<sub>3</sub> (0.1%) and PC/AS<sub>4</sub> (0.08%), respectively. While the control samples of PC/KSS (0.1%) and PC/KSS (0.08%) have the tensile strength of 59.88 MPa and 60.1 MPa, respectively, which are both lower than that of neat PC. As to the flexural test, we see that the flexural strength of PC/AS<sub>3</sub> is slightly decreasing and then increasing with the rise of AS<sub>3</sub> content, while for PC/AS<sub>4</sub>, the

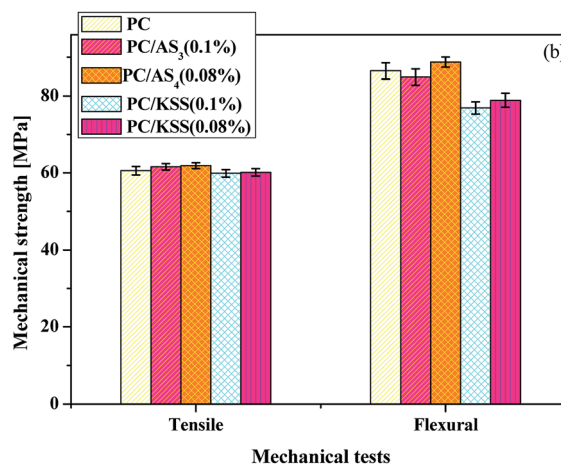
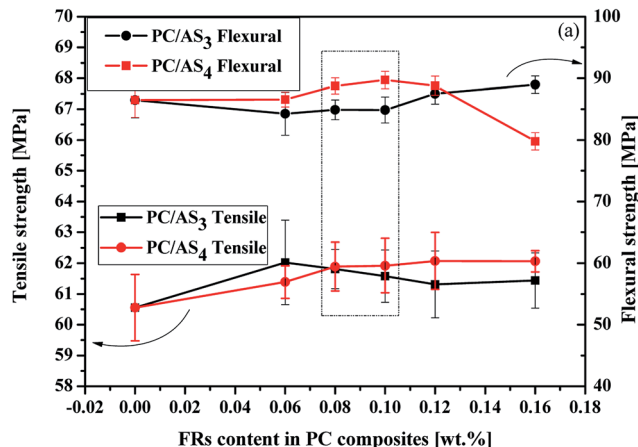


Fig. 6 (a) Effect of the FR content on the mechanical strengths of PC/AS<sub>3</sub> and PC/AS<sub>4</sub> composites; (b) histogram of the mechanical strengths of PC, PC/AS<sub>3</sub> (0.1%), PC/AS<sub>4</sub> (0.08%) and the control samples of PC/KSS (0.1%) and PC/KSS (0.08%).

flexural strength increases first and then decreases sharply. At the optimal addition of each FR for flame retardancy, the flexural strength of PC/AS<sub>3</sub> (0.1%) is 84.87 MPa, slightly reduced by 1.8% compared to that of pure PC of 86.47 MPa, and PC/AS<sub>4</sub> (0.08%) is 88.75 MPa, increased by 2.6% compared to that of PC. In contrast, the flexural strengths are only 76.88 MPa and 78.88 MPa for the control samples of PC/KSS (0.1%) and PC/KSS (0.08%), respectively, which is decreased by 11% than PC.

In conclusion, the novel FR system we proposed in this study can effectively alleviate the deterioration of FR to the mechanical strength of polymeric matrix, and can even improve it to a certain extent in some cases. The advantages of AS<sub>3</sub> and AS<sub>4</sub> FR over the current existing control FR for PC could be attributed to the low incorporated content and the high stiffness and lipid solubility of adamantly that make AS<sub>3</sub> and AS<sub>4</sub> of better compatibility with PC.

### 3.5 Flame retardant mechanism

#### 3.5.1 Thermal decomposition properties of PC composites.

In order to clearly understand the flame retardant mechanism of PC/AS<sub>3</sub> and PC/AS<sub>4</sub>, the thermal stability of the flame



retardant PC composites is investigated by TGA. Moreover, the Flynn–Wall–Ozawa method is used to analyze their thermal degradation kinetics.

Histogram of average activation energy of PC, PC/AS<sub>3</sub> (0.1%), and PC/AS<sub>4</sub> (0.08%) with the degradation conversion rate from 0 to 70% calculated by the Flynn–Wall–Ozawa method.

The thermal degradation and stability of polymers have substantial connection with their flame retardancy. Therefore, TG analysis was used to investigate the thermal degradation properties of PC and its composites. Fig. 7(a) shows the TG and DTG curves under air for the PC, PC/AS<sub>3</sub> (0.1%), and PC/AS<sub>4</sub> (0.08%) composites, respectively. Compared to PC, it is observed that both the TG and DTG curves of PC/AS<sub>3</sub> (0.1%) and PC/AS<sub>4</sub> (0.08%) shift forward to lower temperature successively. The corresponding data such as onset decomposition temperature ( $T_{5\%}$ ), the temperature at maximum weight loss rate ( $T_{\text{peak}}$ ) are list in the insert table of Fig. 7(a). It is found that the  $T_{5\%}$ ,  $T_{\text{peak}}$  of PC are 485.2 °C and 534.2 °C, respectively. However, the  $T_{5\%}$ ,  $T_{\text{peak}}$  are 468.2 °C, 528.8 °C, and 470.4 °C, 521.9 °C for PC/AS<sub>3</sub> (0.1%) and PC/AS<sub>4</sub> (0.08%) respectively. This result is in accordance with the variation of TTI listed in Table 1 that the TTI of the PC/AS<sub>3</sub> and PC/AS<sub>4</sub> composites are shorter than that of virgin PC. It can be deduced that the sulfonate groups in AS<sub>3</sub> or AS<sub>4</sub> flame retardants accelerate the

decomposition of PC and promote its char-forming so as to result in the decline of the degradation temperature as well as TTI. Therefore, the decreased thermal stability is essential rather than a drawback of the multi-sulfonate FR system.

Furthermore, to study the degradation behavior of the PC composites, the Flynn–Wall–Ozawa method is used to analyze their thermal degradation kinetics. According to this method, the degradation activation energy can be determined directly from the  $\log \beta$  versus  $1/T$  plot as follows.<sup>32</sup>

$$\log f(\alpha) = \log \frac{AE}{R} - \log \beta - 2.315 - 0.4567 \frac{E}{RT}$$

where  $A$  is the pre-exponential factor,  $R$  is the gas constant,  $E$  is the activation energy,  $\beta$  is heating rate,  $T$  is the Kelvin temperature, and  $f(\alpha)$  is the integrated form of the conversion dependence function. The TG curves for PC, PC/AS<sub>3</sub> (0.1%), PC/AS<sub>4</sub> (0.08%) composites recorded under various heating flow rates of 5, 10, 15 and 20 °C min<sup>-1</sup> under air atmosphere are shown in Fig. S8–S10.† The activation energy data of the three samples calculated by the Flynn–Wall–Ozawa method are listed in Tables S1–S3,† and the average thermal degradation activation energies within the conversion rate from 0 to 70% are shown in Fig. 7(b). It can be seen clearly from Fig. 7(b) that the average activation energy of PC is 176.9 kJ mol<sup>-1</sup>. When AS<sub>3</sub> or AS<sub>4</sub> is added, the average activation energy decreases to 160.7 kJ mol<sup>-1</sup> and 153.5 kJ mol<sup>-1</sup> for PC/AS<sub>3</sub> (0.1%) and PC/AS<sub>4</sub> (0.08%), respectively. Comparatively, the average activation energy of PC/AS<sub>4</sub> (0.08%) is lower than that of PC/AS<sub>3</sub> (0.1%), which demonstrates stronger accelerating decomposition. This result further manifests that both AS<sub>3</sub> and AS<sub>4</sub> can accelerate PC decomposition. AS<sub>4</sub>, with more sulfonate content in its molecular structure is relatively stronger, which is consistent with TGA results as shown in Fig. 7(a). This could be due to the SO<sub>2</sub> generated from sulfonate degradation which shows high catalytic ability for PC decomposition.

**3.5.2 Morphology and structure analysis of char residue.** In order to further understand the flame retarding mechanism of PC/AS<sub>*n*</sub> system, the morphology and chemical structure of residual char obtained from the sample after LOI test was investigated by SEM and FT-IR, respectively. As can be observed in Fig. 8, the residue char surface of PC is smooth but with macro-pores and crevices, which cannot provide a good barrier for the polymer. In comparison, the char layers of both PC/AS<sub>3</sub> and PC/AS<sub>4</sub> samples are continuous and expansionary with a multitude of expanded spheres. This intumescent char layer provides a good flame shield to stop the propagation of heat and mass to the underneath layer, and delays the volatilization of combustible gases, it also retards the penetration of oxygen, and the feedback of heat. Consequently, such a useful char layer as the flame barrier can make the corresponding PC composites achieve excellent fire retardation.

Fig. 9 shows the FT-IR spectra of virgin PC and the residual char of PC/AS<sub>3</sub> (0.1%) and PC/AS<sub>4</sub> (0.08%), respectively. We can see that the FT-IR spectra for residual char of PC/AS<sub>3</sub> and PC/AS<sub>4</sub> are almost the same, but are of many differences compared to that of the virgin PC. The absorption peak in 3439 cm<sup>-1</sup> and 1400 cm<sup>-1</sup> represents the stretching and plane bending

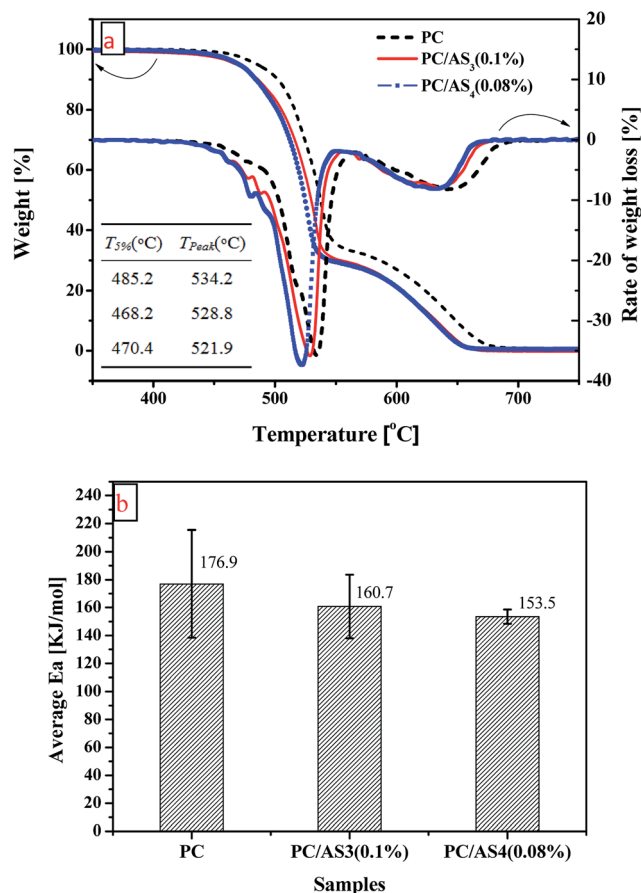


Fig. 7 (a) TG and DTG curves of PC, PC/AS<sub>3</sub> (0.1%), PC/AS<sub>4</sub> (0.08%) composites, (b).





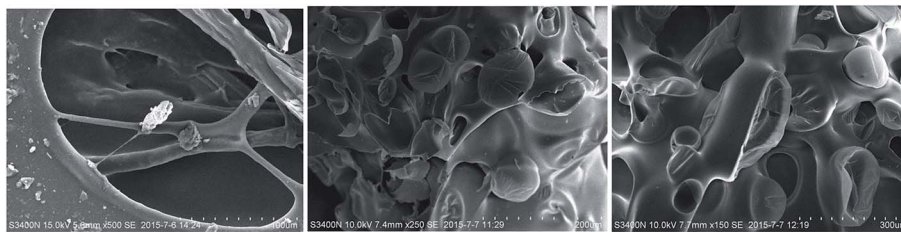


Fig. 8 SEM photos of the residue char for (a) PC, (b) PC/AS<sub>3</sub> (0.1%) and (c) PC/AS<sub>4</sub> (0.08%) composites.

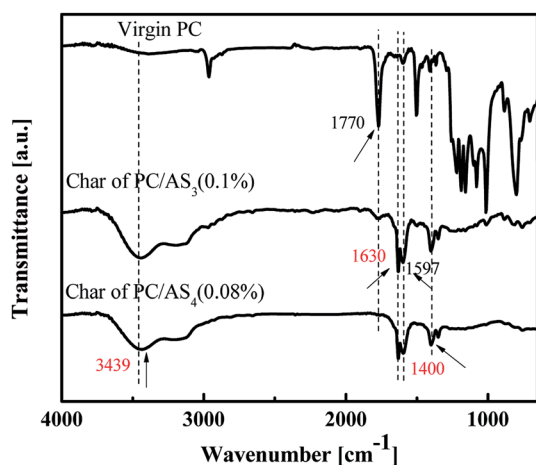


Fig. 9 FT-IR spectra of virgin PC, and the residual char of PC/AS<sub>3</sub> (0.1%) and PC/AS<sub>4</sub> (0.08%).

vibration of  $-OH$  groups, respectively. The characteristic peaks in  $1630\text{ cm}^{-1}$  and  $1597\text{ cm}^{-1}$  are attributed to the  $-C=C-$  in the benzene ring. The above information in FT-IR spectra of residue char for PC/AS<sub>*n*</sub> ( $n = 3, 4$ ) composites indicate that some aromatic alcohol compounds are produced in the residual char of PC/AS<sub>3</sub> or PC/AS<sub>4</sub> after combustion.

From the FT-IR results in combination with the above char morphology and TG analysis of PC and its composites, we can obtain the flame retarding mechanism as follows: the flame retardant AS<sub>3</sub> or AS<sub>4</sub> first decomposes in case of fire and produces SO<sub>2</sub> that serves as a kind of catalyst to accelerate the decomposition of PC. Subsequently, some compounds containing aromatic alcohol are then generated and further cross-linked automatically to promote intumescent char formation, so that the unburned PC is protected with high flame retardancy.

## 4 Conclusions

Two flame retardants (AS<sub>3</sub> and AS<sub>4</sub>) with multi-sulfonate centered on adamantane have been synthesized successfully and characterized by <sup>1</sup>H NMR and FTIR spectra. The TGA results of AS<sub>3</sub> and AS<sub>4</sub> demonstrate that the novel flame retardants have matchable thermal stability with PC matrix. Both the ternary sulfonate AS<sub>3</sub> and the quaternary sulfonate AS<sub>4</sub> exhibit high flame retardant ability to PC. Only 0.1 wt% AS<sub>3</sub> or 0.08 wt% AS<sub>4</sub> can provide PC composites with UL-94 V-0 rating and improve

the LOI value from 25.8% to 31.2% and 32.3% for PC/AS<sub>3</sub> (0.1%) and PC/AS<sub>4</sub> (0.08%), respectively. Moreover, the results from cone calorimetry show that HRR, THR and COY of both PC/AS<sub>3</sub> and PC/AS<sub>4</sub> are reduced compared to the neat PC. In addition, they can maintain good mechanical strength, especially for PC/AS<sub>4</sub> which displays increased mechanical strength in most cases. Finally, we obtain the flame retarding mechanism of this new PC/AS<sub>*n*</sub> system is that AS<sub>3</sub> and AS<sub>4</sub> have a high catalytic effect to accelerate PC thermal degradation and protective char formation. This novel sulfonate flame retardant system provide a new green solution for decreasing the deterioration of the mechanical performance and enhancing the flame retardancy simultaneously.

## Acknowledgements

The authors would like to thank Sun Yat-sen University for plastic processing equipments, Kingfa Sci. and Tech. Co., Ltd. for supporting cone calorimetry tests. In addition, we thank James Wilk who is a English teacher in University of Massachusetts-Amherst for helping us to check the English writing of the revised manuscript. Funding: This work was supported by the National Natural Science Foundation of China [grant numbers 21476051, 21506038 and 21676058], the Nature Science Foundation of Guangdong Province [grant number 2014A030310307], and the Science and Technology Project of Guangdong Province [grant numbers 2013B010403028 and 2016A050502057].

## References

- 1 S. Bourbigot and S. Duquesne, *J. Mater. Chem.*, 2007, **17**, 2283–2300.
- 2 S. Y. Lu and I. Hamerton, *Prog. Polym. Sci.*, 2002, **27**, 1661–1712.
- 3 C. Hoffendahl, G. Fontaine, S. Duquesne, F. Taschner, M. Mezgerb and S. Bourbigot, *RSC Adv.*, 2014, **4**, 20185–20199.
- 4 R. Jeenchan, N. Suppakarn and K. Jarukumjorn, *Composites, Part B*, 2014, **56**, 249–253.
- 5 C. C. Xi, G. Z. Kang, F. C. Lu, J. W. Zhang and H. Jiang, *Mater. Des.*, 2015, **67**, 644–648.
- 6 S. V. Levchik and E. D. Weil, *Polym. Int.*, 2005, **54**, 981–998.
- 7 S. V. Levchik and E. D. Weil, *J. Fire Sci.*, 2006, **24**, 137–151.
- 8 B. Swoboda, S. Buonomo, E. Leroy and J. M. Cuesta Lopez, *Polym. Degrad. Stab.*, 2008, **93**, 910–917.





- 9 Y. H. Guan, W. Liao, Z. Z. Xu, M. J. Chen, J. Q. Huang and Y. Z. Wang, *RSC Adv.*, 2015, **5**, 59865–59873.
- 10 Q. X. He, L. Tang, T. Fu, Y. Q. Shi, X. L. Wang and Y. Z. Wang, *RSC Adv.*, 2016, **6**, 52485–52494.
- 11 T. Yu, T. Tuerhongjiang, C. Sheng and Y. Li, *Composites, Part A*, 2017, **97**, 60–66.
- 12 M. Rajaei, D. Y. Wang and D. Bhattacharyya, *Composites, Part B*, 2017, **113**, 381–390.
- 13 L. Dang, X. Nai, Y. Dong and W. Li, *RSC Adv.*, 2017, **7**, 21655–21665.
- 14 W. C. Zhang, X. M. Li, H. B. Fan and R. J. Yang, *Polym. Degrad. Stab.*, 2012, **97**, 2241–2248.
- 15 J. P. Ding, Z. Q. Tao, X. B. Zuo, L. Fan and S. Y. Yang, *Polym. Bull.*, 2009, **62**, 829–841.
- 16 X. P. Hu, Y. Y. Guo, L. Chen, X. L. Wang, L. J. Li and Y. Z. Wang, *Polym. Degrad. Stab.*, 2012, **97**, 1772–1778.
- 17 L. Li, P. Wei, J. Li, J. Jow and K. Su, *J. Fire Sci.*, 2010, **28**, 523–538.
- 18 Z. Hu, L. Chen, B. Zhao, Y. Luo, D. Y. Wang and Y. Z. Wang, *Polym. Degrad. Stab.*, 2011, **96**, 320–327.
- 19 R. K. Jian, L. Chen, Z. Hu and Y. Z. Wang, *J. Appl. Polym. Sci.*, 2012, **123**, 2867–2874.
- 20 W. Zhao, B. Li, M. Xu, K. Yang and L. Lin, *Fire Mater.*, 2013, **37**, 530–546.
- 21 K. H. Pawlowski and B. Schartel, *Polym. Int.*, 2007, **56**, 1404–1414.
- 22 L. Duan, H. Yang, L. Song, Y. Hou, W. Wang, Z. Gui and Y. Hu, *Polym. Degrad. Stab.*, 2016, **134**, 179–185.
- 23 Z. J. Jiang, S. M. Liu, J. Q. Zhao and X. B. Chen, *Polym. Degrad. Stab.*, 2013, **98**, 2765–2773.
- 24 S. Q. Fu, J. W. Guo, D. Y. Zhu, Z. Yang, C. F. Yang, J. X. Xian and X. Li, *RSC Adv.*, 2015, **5**, 67054–67065.
- 25 S. B. Nie, Y. Hu, L. Song, S. Q. He and D. D. Yang, *Polym. Adv. Technol.*, 2008, **19**, 489–495.
- 26 Y. Z. Wang, B. Yi, B. Wu, B. Yang and Y. Liu, *J. Appl. Polym. Sci.*, 2003, **89**, 882–889.
- 27 A. Nodera and T. Kanai, *J. Appl. Polym. Sci.*, 2004, **94**, 2131–2139.
- 28 S. M. Liu, H. Ye, Y. S. Zhou, J. H. He, Z. J. Jiang, J. Q. Zhao and X. B. Huang, *Polym. Degrad. Stab.*, 2006, **91**, 1808–1814.
- 29 H. Newman, *Synthesis*, 1972, **12**, 692–693.
- 30 A. Genovese and R. A. Shanks, *Composites, Part A*, 2008, **39**, 398–405.
- 31 W. Y. Xing, W. Yang, W. J. Yang, Q. H. Hu, J. Y. Si, H. D. Lu, B. H. Yang, L. Song, Y. Hu and R. K. K. Yuen, *ACS Appl. Mater. Interfaces*, 2016, **39**, 26266–26274.
- 32 Q. X. He, L. Tang, T. Fu, Y. Q. Shi, X. L. Wang and Y. Z. Wang, *RSC Adv.*, 2016, **6**, 52485–52494.

